

# Numerical investigation on gypsum and ettringite formation in cement pastes subjected to sulfate attack

Xiao-Bao Zuo<sup>\*1</sup>, Jia-Lin Wang<sup>1</sup>, Wei Sun<sup>2</sup>, Hua Li<sup>2</sup> and Guang-Ji Yin<sup>1</sup>

<sup>1</sup>Department of Civil Engineering, Nanjing University of Science & Technology, Nanjing 210094, China  
<sup>2</sup>Jiangsu Key Laboratory of Construction Materials, Southeast University, Nanjing 211189, China

(Received October 30, 2015, Revised October 13, 2016, Accepted October 15, 2016)

**Abstract.** This paper uses modelling and experiment to perform a quantitative analysis for the gypsum and ettringite formations in cement pastes subjected to sulfate attack. Firstly, based on Fick's law and chemical reaction kinetics, a diffusion model of sulfate ions in cement pastes is proposed, and then the model of the gypsum and ettringite formations is established to analyze its contents in cement pastes with corrosion time. Secondly, the corrosion experiment of the specimens with cement pastes immersed into 2.5%, 5.0% and 10.0% Na<sub>2</sub>SO<sub>4</sub> solutions are carried out, and by using XRD-Rietveld method, the phases of powder samples from the specimens are quantitatively analyzed to obtain the contents of gypsum and ettringite in different surface depth, solution concentration and corrosion time. Finally, the contents of gypsum and ettringite calculated by the models are compared with the results from the XRD experiments, and then the effects of surface depth, corrosion time and solution concentration on the gypsum and ettringite formations in cement pastes are discussed.

**Keywords:** model; XRD-Rietveld analysis; gypsum; ettringite; cement pastes; sulfate attack

## 1. Introduction

The deterioration of cement-based materials caused by sulfate attack is a major threat to the durability of concrete structures exposed permanently to the sulfate environments, such as sea water, groundwater, decaying organic matter, and industrial effluent (Sun and Yu 2001, Monteiro and Kurtis 2003, Yang *et al.* 2005, Liu *et al.* 2014). Sulfate attack on cement-based materials is a very complicated process (Santhannam *et al.* 2001, Neville 2004). Despite some controversy on the deterioration mechanisms of cement-based materials caused by sulfate attack, the main viewpoint is that the deterioration is associated with both of the diffusion of sulfate ions in cement-based materials and the chemical reactions between sulfate ions and the hydrated products to form gypsum and ettringite (Neville 2004, Santhannam *et al.* 2003, Guneyisi *et al.* 2010, Xiong *et al.* 2015). The formation of gypsum and ettringite are accompanied with volume expansion, spalling, cracking, softening of cement pastes, and inducing the tension stress in the microstructures of materials (Tian and Cohen 2000, Lothenbach *et al.* 2010, Rahman and Bassuoni 2014), which cause the deterioration of the physical and mechanical properties of cement-based materials such as strength and stiffness (Shazali *et al.* 2006, Schmidt *et al.* 2009, Guneyisi *et al.* 2010, Sarkar *et al.* 2010, Kalipcilar *et al.* 2016).

Thus, numerical investigation on the formations of gypsum and ettringite in cement-based materials is very

necessary for further analysis of the durability deterioration of concrete structures subjected to sulfate attack.

There are two basic problems to numerically investigate the formations of gypsum and ettringite in cement-based materials subjected to sulfate attack: the modeling of the diffusion process of sulfate ions and the quantification of the formation process of gypsum and ettringite. Various aspects of the first problem have already been studied by researchers, and they have applied Fick's law for setting up some models to characterize the diffusion process of sulfate ions in cement-based materials (Samson *et al.* 1999, Tixier and Mobasher 2003, Gospodinov 2005, Zuo *et al.* 2012c). In these models, not only the diffusivity of sulfate ion but also the kinetics of the reactions between sulfate ions and the hydrate products need to be considered, this is because the sulfate ion dissipation caused by the chemical reactions has a significant influence on the diffusion process. The diffusivity of sulfate ions in cement-based materials has presently attracted more attention, but the reaction kinetics is mainly attributable to the first order reaction between sulfate ion and calcium hydroxide (Clifton *et al.* 1994). Most studies of the second problem are focused on the expansion mechanisms caused by the gypsum and ettringite formation (Sarkar *et al.* 2010, Rahman and Bassuoni 2014). Some studies have been carried out to observe the alteration of the phases of hydrated cement in the process of sulfate attack by using Scanning Electron Microscopy, SEM (Gollop and Taylor 1992, Diamond and Lee 1999, Brown *et al.* 2004), and describe the morphology of gypsum and ettringite in the regions close to the material surface (Bonen 1992, Santhannam *et al.* 2003). The other studies have also used the XRD and SEM to investigate the influences of sulfate attack on the microstructures of cement hydrated products, and make a confirmation that the expansion

---

\*Corresponding author, Ph.D.  
E-mail: [xbzuo@sina.com](mailto:xbzuo@sina.com)

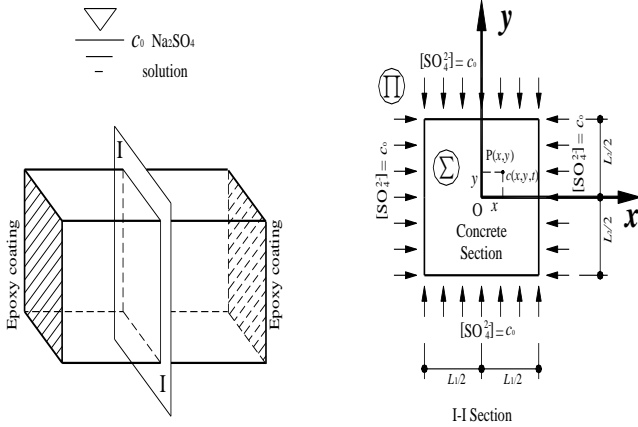


Fig. 1 Diffusion model of sulfate ions in the prismatic specimen

mechanism in cement pastes is related to the ettringite formation, which occur in the region of the highly localized gypsum formation (González and Irassar 1997). These studies have explained the qualitative formation and expansion mechanism of gypsum and ettringite in cement-based materials under sulfate attack, but the time-varied formation of gypsum and ettringite have not been further quantitatively investigated to characterize the evolution of sulfate expansion in cement-based materials. Thus, a general framework, which can conjugate two problems in an integrative model to predict quantitatively the formations of gypsum and ettringite in cement-based materials, should be further developed. These models may help researchers and engineers to study the durability deterioration of concrete structures.

This paper presents a quantitative description of the gypsum and ettringite formation, which are related to the diffusion of sulfate ions and chemical reaction of gypsum and ettringite formation, for predicting the time-varied formation processes of gypsum and ettringite in the specimens immersed into  $\text{Na}_2\text{SO}_4$  solutions. For that, an integrative model for the diffusion process of sulfate ion and the kinetics of gypsum and ettringite formation in cement pastes is suggested. Then, the corrosion experiments of the specimens under the different concentrations of  $\text{Na}_2\text{SO}_4$  solution are carried out, and X-ray diffraction with the full profile Rietveld method (XRD-R) is used for the quantitative phase analysis on the powder samples from the corroded specimens. Finally, an integrative model is validated with the results from the X-ray microanalysis, and the effects of the surface depth, the solution concentration and the corrosion time on the formation of gypsum and ettringite in the cement pastes are discussed.

## 2. Model

### 2.1 Diffusion of sulfate ions

The formation of gypsum and ettringite is related to the diffusion of environmental sulfate ions in the cement-based materials (Young 1998), so modeling the diffusion process

is necessary for calculating the formation of gypsum and ettringite. The object of this study is a prismatic specimen with cement pastes subjected to  $\text{Na}_2\text{SO}_4$  solutions, two ends of which are sealed with the epoxies, as shown in Fig. 1. Due to the coexistence of the ionic diffusion and chemical reaction, the diffusion process of sulfate ions in the prism can be obtained by using Fick's second law and chemical reaction kinetics (Laidler 1987), which can be expressed by

$$\begin{cases} \frac{\partial c}{\partial t} = \frac{\partial \left( D_c \frac{\partial c}{\partial x} \right)}{\partial x} + \frac{\partial \left( D_c \frac{\partial c}{\partial y} \right)}{\partial y} + \frac{\partial C_d}{\partial t} \\ c(x, y, 0) = 0, \quad (x, y) \in \Omega \\ c(L_1/2, y, t) = c_0, \quad c(x, L_2/2, t) = c_0 \\ c(-L_1/2, y, t) = c_0, \quad c(x, -L_2/2, t) = c_0 \end{cases} \quad (1)$$

Where  $c=c(x, y, t)$  is the concentration of sulfate ion at the point  $(x, y)$  at the time  $t$ ,  $t$  is the diffusion time,  $C_d=C_d(x, y, t)$  is the sulfate ion concentration dissipated by the chemical reaction to form the gypsum,  $c_0$  is the environmental sulfate ion concentration,  $L_1$  and  $L_2$  are the across section dimensions of specimen along the  $x$  and  $y$  directions respectively,  $\Omega$  is the cross sectional area of the specimen,  $D_c$  is the diffusion coefficient of sulfate ion in cement pastes, as given in Eq. (2).

#### 2.1.1 Diffusion coefficient

The diffusivity of sulfate ion has a significant influence on the gypsum and ettringite formation in cement-based materials, and the diffusion coefficient in cement pastes is related to its microstructure (mainly including porosity and tortuosity) (Garboczi 1990, Zhang *et al.* 2011) and the ionic concentration (such as ionic strength and conductivity of pore solution) (Samson *et al.* 1999). The diffusion coefficient of sulfate ion in cement paste is a time- and space-varied functions associated with the sulfate ion concentration. Based on the electrolyte solution theories such as Davis model and Mode coupling theory treatment of the electrolyte friction (Samson *et al.* 1999, Chandra and Bagchi 1999), the diffusion coefficient of sulfate ion, considering the influence of the ionic concentration on its diffusivity, can be expressed as (Zuo, Sun *et al.* 2010d)

$$D_c = \frac{\varphi_{cp} RT}{4\tau_{cp} F^2} \left[ \Lambda^0 - (1.073 \times 10^{-5} + 0.01 \Lambda^0) \sqrt{c} \right] \quad (2)$$

Where  $R=8.314 \text{ J} \cdot \text{K}^{-1} \cdot \text{mol}^{-1}$  is the gas constant,  $T$  is the environmental temperature, K,  $F=96480 \text{ J} \cdot \text{K}^{-1} \cdot \text{mol}^{-1}$  is the Faraday constant,  $\Lambda^0=8.0 \times 10^{-3} \text{ Sm}^2/\text{mol}$  is the conductivity of sulfate ion,  $\varphi_{cp}$  and  $\tau_{cp}$  is the pore-filled cement paste porosity and tortuosity respectively.

#### 2.1.2 Porosity

Porosity is an important parameter reflecting on the microstructures of cement-based materials and influencing the ionic diffusivity. In the process of sulfate attack, the pores are gradually filled with the chemical products, and the porosity decreases with the formation of chemical products, which generate a gradient distribution from the surface to the interior of specimen, so the porosity will vary

with the spatial position and corrosion time. Considering the filling of the pores, the porosity of the cement paste specimen can be calculated using

$$\varphi_{cp} = \varphi_{cp0} - \phi_{prod} \quad (3)$$

Where  $\varphi_{cp}$  is the time- and space- varied porosity,  $\varphi_{cp0}$  is the initial porosity without considering the filling of pores by the chemical products, and it is expressed as (Clifton *et al.* 1994)

$$\varphi_{cp0} = \frac{w_c - 0.39h_\alpha}{w_c + 0.32} \quad (4)$$

$w_c$  is the water-cement ratio,  $h_\alpha$  denotes the cement hydration degree.  $\phi_{prod}$  is the porosity filled by the chemical products such as gypsum and ettringite (Santhanam *et al.* 2003). The gypsum and ettringite are plates and hexagonal needle crystals respectively, and their growth will result in the honeycombed distribution in the pores (González and Irassar 1997, Yan *et al.* 2001), so the pores cannot be fully filled with the gypsum and ettringite. In general, when the pores are filled with gypsum and ettringite to 70-90 percent of the total initial porosity, the expansion will be produced (Tixier and Mobasher 2003). In order to simplify the calculation of the pore-filled porosity ( $\phi_{prod}$ ), the filling of gypsum and ettringite is assumed to be equivalent to the ettringite formation, so the pore-filled porosity ( $\phi_{prod}$ ) associated with the feature of gypsum and ettringite filling in the pores can be determined by (Zuo *et al.* 2012b)

$$\phi_{prod} = 5.876 \times 10^{-3} c_{Ett} \quad (5)$$

Where  $c_{Ett}$  is the concentration of ettringite in the specimen, as given in the following Eq. (18).

### 2.1.3 Tortuosity

Tortuosity is a very important pore structure parameter of the cement paste (Coleman 2008), and it plays a fundamental role in governing the transport processes that influence the durability-based performance of cement-based materials (Yoon 2009, Stroeven 2000). Based on the compositions and geometric features of the cement pastes, a geometrical approach is used to obtain a model for the tortuosity of transport paths in the cement paste, and it can be expressed as (Zuo *et al.* 2012, Zuo *et al.* 2014)

$$\tau_{cp} = \omega_{wc} \eta_r h_\alpha \left[ \frac{1}{1 - \sqrt{1 - \varphi_{cp}}} \sqrt{\left(1 - \sqrt{1 - \varphi_{cp}}\right)^2 + \frac{1}{4}} \right] \quad (6)$$

Where  $\omega_{wc}$  is the adjustment coefficient associated with the water-cement ratio,  $\eta_r$  is the shape factor of hydrated cement particles.

## 2.2 Formation of gypsum and ettringite

### 2.2.1 Chemical reaction

Based on the mechanism of sulfate attack on cement-based materials (Monteiro and Kurtis 2003, Santhanam *et al.* 2003, Rahman and Bassuoni 2014), the formations of gypsum and ettringite are associated with the chemical

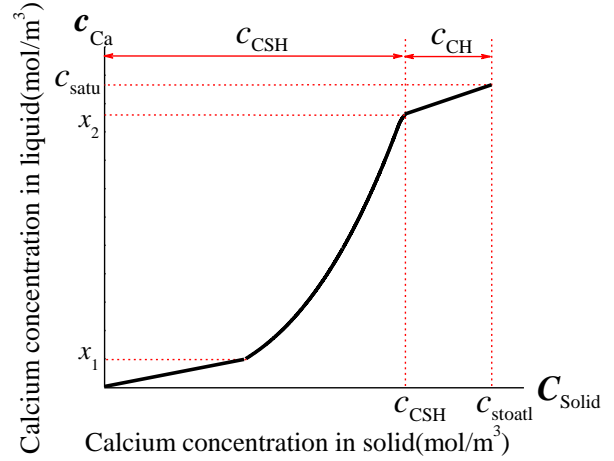
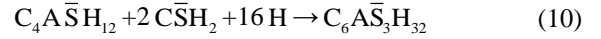
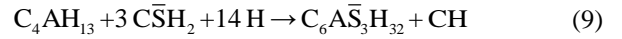
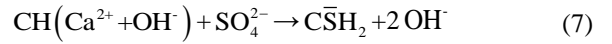


Fig. 2 Curve describing equilibrium between calcium ions concentrations in the pore

reaction between the sulfate ions and the cement hydration products, and the process may be expressed by the following chemical reactions



For the convenience of calculation, Eqs. (8)-(10) may be briefly replaced by



Where CA refers to the calcium aluminates,  $q$  is the equivalent reaction coefficient of the gypsum dissipation to produce ettringite (Tixier and Mobasher 2003).

### 2.2.2 Dissipation of sulfate ions

The gypsum formation may be calculated by the sulfate ion concentration dissipated by chemical reaction in Eq. (7), which can be regarded as a second-order reaction in the pore solution. Based on the chemical reaction kinetics (Laidler 1987, Zang 1995), the sulfate ion concentration dissipated by the chemical reaction, namely the second term in the right-hand-side of Eq. (1), can be expressed by

$$\frac{\partial C_d}{\partial t} = -k_v \cdot c_{Ca} \cdot c \quad (12)$$

Where  $k_v$  is the chemical reaction rate constant in Eq. (7),  $c_{Ca}$  is the calcium ion concentration in the pore solution.

By the integration of Eq. (12) over the time (0,  $t$ ), the sulfate ion concentration  $C_d$  dissipated by the chemical reaction in cement pastes can be calculated by

$$C_d = \int_0^t (-k_v \cdot c_{Ca} \cdot c) dt \quad (13)$$

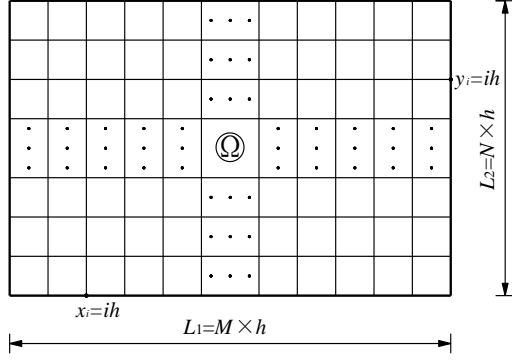


Fig. 3 Mesh

### 2.2.3 Concentration of calcium ions in pore solution

In the process of sulfate attack, the calcium ions in pore solutions are continuously dissipated by chemical reaction in Eq. (7). The reduction of the calcium ion concentration can cause the dissolution of calcium hydroxide (CH) and calcium silicate hydrate (CSH) gel (Mainguy *et al.* 2000, Kamali *et al.* 2008, Wee 2001, Sarkar *et al.* 2012). Assuming a chemical equilibrium between calcium ion concentrations in the solid phases (CH and CSH) and in the pore solution, the solid-liquid equilibrium relationship for calcium may be described by a phenomenological chemistry model (Gerard *et al.* 2002, Wan *et al.* 2013), as shown in Fig. 2, which may be expressed by

$$c_{Ca} = \begin{cases} \frac{c_{satu} - x_2}{c_{CH}} (c_s - c_{CSH}) + x_2 & c_{CSH} \leq c_s \leq (c_{CSH} + c_{CH}) \\ c_{satu} \left( \frac{c_s}{c_{CSH}} \right)^3 & c_{CSH} \left( \frac{x_1}{c_{satu}} \right)^{\frac{1}{3}} \leq c_s \leq c_{CSH} \\ \left( x_1^2 c_{satu} \right)^{\frac{1}{3}} \frac{c_s}{c_{CSH}} & 0 \leq c_s \leq c_{CSH} \left( \frac{x_1}{c_{satu}} \right)^{\frac{1}{3}} \end{cases} \quad (14)$$

Where  $c_{CSH}$  is the calcium concentration in the CSH gel, and  $c_{CH}$  is the calcium concentration in the CH phase, both of them in cement-based materials are measured by the XRD-Rietveld method (Scrivener *et al.* 2004).  $c_{satu}$  is the saturated calcium ion concentration,  $c_s$  is the total calcium concentration in the solid phase (CH and CSH), and it can be calculated by the previous sulfate ion concentration  $C_d$  dissipated by the chemical reaction in Eq. (7):  $c_s = c_{CH} + c_{CSH} + C_d$ .  $x_1$  is the calcium ion concentration in the liquid below which no CSH gel exists, and  $x_2$  is the calcium ion concentration at which CH has completely dissolved. For computational ease,  $x_2$  is taken as  $(c_{satu} - 3)$  mol/m<sup>3</sup> (Nakarai *et al.* 2006).

### 2.2.4 Concentration of gypsum and ettringite

Known from the chemical reaction Eq. (7), the total gypsum formation in cement pastes, is equal to the sulfate ion concentration  $C_d$  dissipated by chemical reaction, and the parts of gypsum are dissipated by the chemical reactions with the calcium aluminates to produce ettringite, as shown in Eqs. (8)-(11), but the chemical reactions between calcium aluminates and gypsum are the complicated solid-solid reactions. Based on the principle of the solid-solid reactions

(Suresh and Ghoroi 2009), the chemical reaction kinetic equation in Eq. (11) may be expressed by

$$\begin{cases} \frac{\partial c_{CA}}{\partial t} = -k_{v1} \cdot c_{CA}^{\alpha} \cdot c_{Gyp}^{\beta} \\ c_{CA}(x, 0) = c_{CA0} \end{cases} \quad (15)$$

Where  $c_{CA}$  is the concentration of calcium aluminates in cement pastes,  $C_{Gyp}$  is the concentration of gypsum in cement pastes,  $k_{v1}$  is the chemical reaction rate constant,  $t$  refers to the diffusion-reaction time,  $c_{CA0}$  is the initial concentration of calcium aluminates in cement pastes,  $\alpha$  and  $\beta$  are the chemical reaction order of calcium aluminates and gypsum respectively, which can be obtained by the experiment of reaction kinetics (Zang 1995).

In the diffusion-reaction process, the dissipation of calcium aluminates caused by the ettringite formation in cement pastes can be calculated by  $(c_{CA0} - c_{CA})$ . Based on the stoichiometric reaction in Eq. (10), the concentration of gypsum dissipated by the ettringite formation in cement pastes is  $q(c_{CA0} - c_{CA})$ . Thus, in the process of the ettringite formation, the real concentration of gypsum should be a difference between the total amount of gypsum formed ( $C_d$ ) and the concentration of gypsum dissipated,  $q(c_{CA0} - c_{CA})$

$$c_{Gyp} = C_d - q(c_{CA0} - c_{CA}) \quad (16)$$

Substituting Eq. (16) into Eq. (15), it can be obtained that

$$\begin{cases} \frac{\partial c_{CA}}{\partial t} = -k_{v1} \cdot c_{CA}^{\alpha} \cdot [C_d - q(c_{CA0} - c_{CA})]^{\beta} \\ c_{CA}(x, 0) = c_{CA0} \end{cases} \quad (17)$$

According to the stoichiometric reaction in Eq. (11), the formation of ettringite in cement pastes is equivalent to the dissipation of calcium aluminates, namely

$$c_{Ett} = c_{CA0} - c_{CA} \quad (18)$$

In the above Eqs. (1), (13), (14), (16)-(18), Eqs. (1) and (14) are used to calculate the concentrations of sulfate ion ( $c$ ) and calcium ion in cement pastes ( $c_{Ca}$ ) respectively. The sulfate ion concentration ( $C_d$ ) dissipated by chemical reaction in cement pastes can be calculated using Eq. (13), and by the numerical solution of Eq. (17), the concentration of calcium aluminates in cement pastes ( $c_{CA}$ ) can be obtained. Finally, using Eqs. (16) and (18), the concentrations of gypsum and ettringite in the cement paste may be calculated. The above differential equations in Eqs. (1), (12) and (17) are numerically solved by the Finite Different Method with Alternating Direction Implicit scheme (ADI) (Sun 2005, Zuo *et al.* 2012c).

## 2.3 Numerical approaches

### 2.3.1 Mesh

In order to solve the diffusion-reaction Eq. (1) to obtain the formation of gypsum and ettringite, the cross-sectional area  $\Omega(L_1 \times L_2)$  of specimen is meshed with the same space  $h$

Table 1 Chemical composition of ordinary Portland cement (CEM I 52.5)

Mineral components (mass %)	C <sub>3</sub> S	C <sub>2</sub> S	C <sub>3</sub> A	C <sub>4</sub> AF	Gypsum
	55.5	19.1	6.5	10.1	5
Chemical compositions (mass %)	SiO <sub>2</sub>	Al <sub>2</sub> O <sub>3</sub>	C <sub>a</sub> O	M <sub>g</sub> O	SO <sub>3</sub>
	21.35	4.67	62.60	3.08	2.25
	Fe <sub>2</sub> O <sub>3</sub>	Na <sub>2</sub> O	K <sub>2</sub> O	LOI	Others
	3.31	0.21	0.54	0.95	1.04

along both of  $L_1$  and  $L_2$ , as shown in Fig. (3), and the time interval is selected as  $\Delta t$ . Two clusters of the parallel lines are defined:  $x_i=ih$  ( $i=0, 1, 2, \dots, i, \dots, M$ ;  $M$  is the number of grid in the  $x$  direction),  $y_j=jh$  ( $j=0, 1, 2, \dots, j, \dots, N$ ;  $N$  is the number of grid in the  $y$  direction), and  $t_k=k\Delta t$  ( $k=0, 1, \dots, k, \dots, K$ ;  $K$  is the number of diffusion time). The section area  $\Omega$  is divided into square grids ( $M \times N$ ), and the grid nodes are  $(x_i, y_j, t_k)$ . Thus, the concentration of sulfate ion, calcium ion, gypsum and ettringite at the state  $(x_i, y_j, t_k)$  may be expressed by  $c_{ij}^k, c_{Ca_{ij}}^k, c_{Gyp_{ij}}^k, c_{Ett_{ij}}^k$ .

### 2.3.2 Iterative solutions from ADI difference scheme

Eq. (1) is a nonlinear partial differential equation, and it can be solved by the finite different method with Alternating Direction Implicit scheme, ADI (Sun 2005), in which the transition time  $t_{k+1/2}$  is used to divide the time interval ( $t_k, t_{k+1}$ ) into two intervals, ( $t_k, t_{k+1/2}$ ) and ( $t_{k+1/2}, t_{k+1}$ ). The solving process of Eq. (1) is divided into two steps to obtain the iterative solution of sulfate ion concentration in Eq. (1).

The first step, at the interval ( $t_k, t_{k+1/2}$ ), using the implicit and explicit scheme in the  $x$  and  $y$  directions respectively. The iterative solutions of Eq. (1) at the time  $t_{k+1/2}$  can be obtained by

$$\{c_j^{k+1/2}\} = [A']^{-1} [B' \{c_{j-1}^k\} + C' \{c_{j+1}^k\} + D' \{c_j^k\} + \{e'\}] \quad (19)$$

The second step, at the interval ( $t_{k+1/2}, t_{k+1}$ ), using the explicit and implicit scheme in the  $x$  and  $y$  directions respectively, the iterative solutions of Eq. (1) at the time  $t_{k+1}$  can be expressed by

$$\{c_i^{k+1}\} = [A'']^{-1} [B'' \{c_{i-1}^{k+1/2}\} + C'' \{c_{i+1}^{k+1/2}\} + D'' \{c_i^{k+1/2}\} + \{e''\}] \quad (20)$$

In Eqs. (19) and (20),  $\{c_j^{k+1/2}\}$  refers to  $M \times 1$  order vector, which represents the concentrations of sulfate ions at points  $(x_i, y_j; i=1, 2, \dots, M)$  at the time  $t_{k+1/2}$ ;  $\{c_i^{k+1}\}$  refers to  $N \times 1$  order vector, which is the concentrations of sulfate ions at every points  $(x_i, y_j; j=1, 2, \dots, N)$  at the time  $t_{k+1}$ . The other matrix and vectors in Eqs. (19) and (20) are presented in Appendix A.

Using the Chasing method to solve the combination of Eqs. (19) and (20), the numerical solutions of Eq. (1) at the time intervals ( $t_k, t_{k+1}$ ), namely the sulfate ion concentrations  $c_{ij}^{k+1}$  at the points  $(x_i, y_j)$  and the time  $t_{k+1}$ , can be obtained.

After numerical discretization, and considering the initial concentration of sulfate ions dissipated is zero, Eq.

(16) can be changed into a numerical model, which is expressed as

$$\begin{cases} C_{dij}^{k+1} = C_{dij}^k - k_v c_{Ca_{ij}}^k c_{ij}^{k+1} \Delta t \\ C_{dij}^1 = 0 \end{cases} \quad (21)$$

In Eq. (21), the concentration of calcium ion  $c_{Ca_{ij}}^k$  may be determined by Eq. (14). Substituting sulfate ion concentration  $c_{ij}^{k+1}$  calculated by ADI difference scheme and calcium ion concentration  $c_{Ca_{ij}}^k$  in Eq. (14) into Eq. (21), the accumulative concentration of sulfate ions  $C_{dij}^{k+1}$  dissipated in the cement pastes can be obtained.

By discretizing the kinetics Eq. (17), the calcium aluminate concentration  $c_{CA_{ij}}^{k+1}$  can be expressed by

$$\begin{cases} c_{CA_{ij}}^{k+1} = c_{CA_{ij}}^k - k_{v1} [c_{CA_{ij}}^k]^\alpha [C_{dij}^{k+1} - q(c_{CA0} - c_{CA_{ij}}^k)]^\beta \Delta t \\ c_{CA_{ij}}^1 = c_{CA0} \end{cases} \quad (22)$$

Placing the accumulative concentration of sulfate ions  $C_{dij}^{k+1}$  dissipated in Eq. (21), the concentration of the calcium aluminates  $c_{CA_{ij}}^{k+1}$  in the cement pastes can be obtained by the iterative solution at every time in Eq. (22)

Thus, numerically discretizing Eqs. (16) and (18) of gypsum and ettringite formation

$$c_{Gyp_{ij}}^{k+1} = C_{dij}^{k+1} - q(c_{CA0} - c_{CA_{ij}}^{k+1}) \quad (23)$$

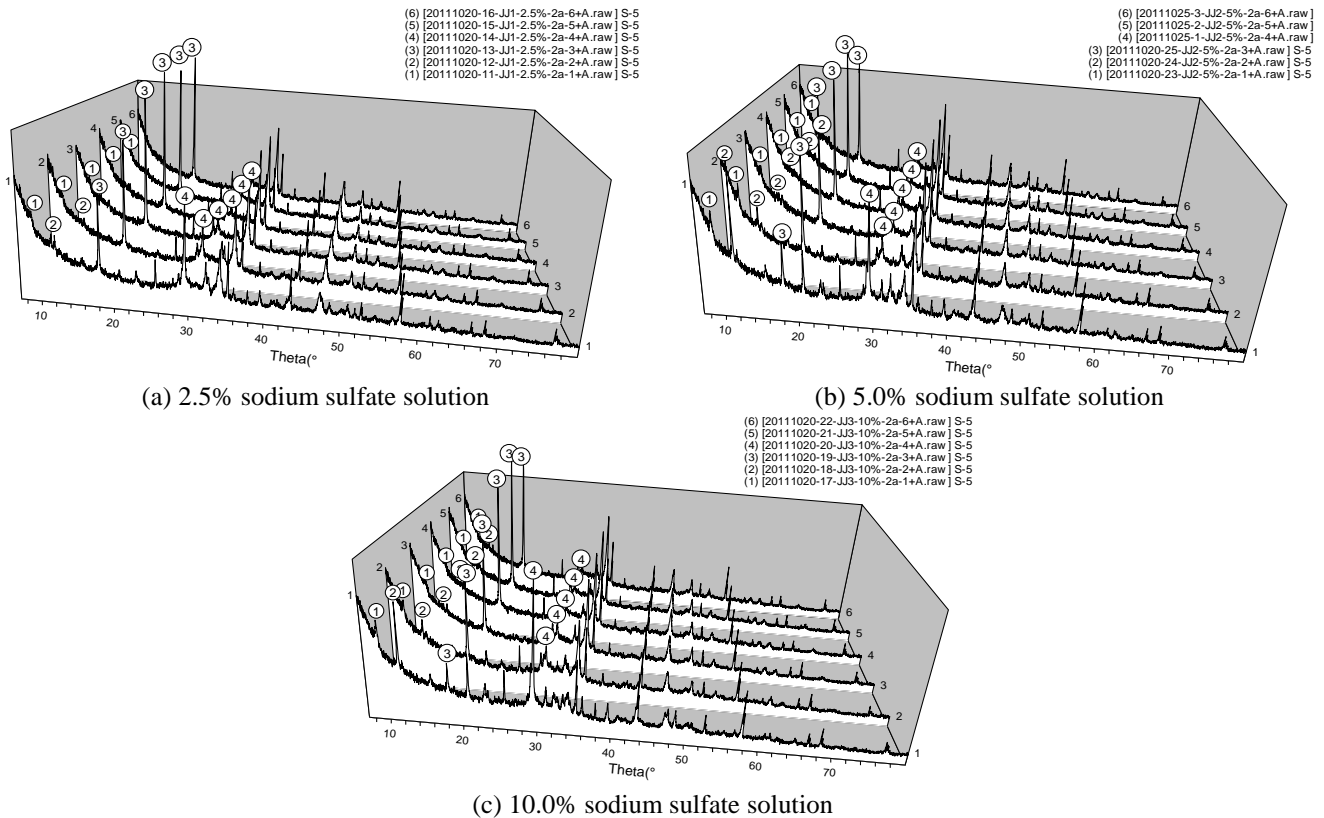
$$c_{Ett_{ij}}^{k+1} = C_{CA_{ij}}^{k+1} - c_{CA0} - c_{CA_{ij}}^{k+1} \quad (24)$$

And placing the concentration of the calcium aluminates  $c_{CA_{ij}}^{k+1}$  in Eq. (22) and the concentration of sulfate ions dissipated  $C_{dij}^{k+1}$  in Eq. (21) into Eqs. (23) and (24) respectively, the concentration of gypsum and ettringite formation at every time can be obtained by numerical iteration. Therefore, Based on the above proposed models and calculating process, and using MATLAB language, the computing programme NIFGESA.M have been completed to investigate numerically the formation of gypsum and ettringite in cement pastes caused by the environmental sulfate attack.

## 3. Experiments

### 3.1 Materials and specimen

The cement used in this study is an ordinary Portland cement (CEM I 52.5), and its mineral and chemical compositions are presented in Table 1. The density of the cement is 3150 kg/m<sup>3</sup>, and its specific surface area is 369.6 m<sup>2</sup>/kg. The pure cement pastes were mixed at water-cement ratio of 0.35, and its normal compression strength and flexural strength for curing 28 days are 60.5 MPa and 8.7 MPa, respectively.



Number in figure	1	2	3	4	5	6
Powder sample	0-1 mm	1-2 mm	2-4 mm	4-6 mm	6-8 mm	8-10 mm

Fig. 4 XRD patterns of powder samples at every layer of specimen under different concentrations of  $\text{Na}_2\text{SO}_4$  solutions at 720 days (①-Ettringite, ②-Gypsum, ③-Calcium hydroxide, ④-Calcite)

Cement paste specimens with  $40 \times 40 \times 160 \text{ mm}^3$  prism were cast according to the mixtures of water and cement with the water/cement ratio 0.35, and they are cured in  $20^\circ\text{C}$  water. After 24 hours, the pure paste specimens were demoulded and continue to be cured in a standard curing room (temperature,  $20 \pm 2^\circ\text{C}$ ; relative humidity, over 95%) for 57 days before the corrosion experiments.

Before being immersed into the  $\text{Na}_2\text{SO}_4$  solutions, the two end surfaces with dimension  $40 \text{ mm} \times 40 \text{ mm}$  of the specimens were sealed with a low viscosity of the epoxy resin, and the other four surfaces with dimension  $40 \text{ mm} \times 160 \text{ mm}$  were polished to remove uniformly the thin layer of cement pastes. After being saturated for 2 days (total 60 days curing), all of the specimens were immediately immersed into 2.5%, 5.0% and 10.0% by mass of  $\text{Na}_2\text{SO}_4$  solutions respectively. The  $\text{Na}_2\text{SO}_4$  solutions were replaced at every three months to maintain a constant corrosion environment, and the containers filled with the specimens and solutions were placed in the room temperature and closed to protect from carbonation.

### 3.2 Preparation of X-ray diffraction powder samples

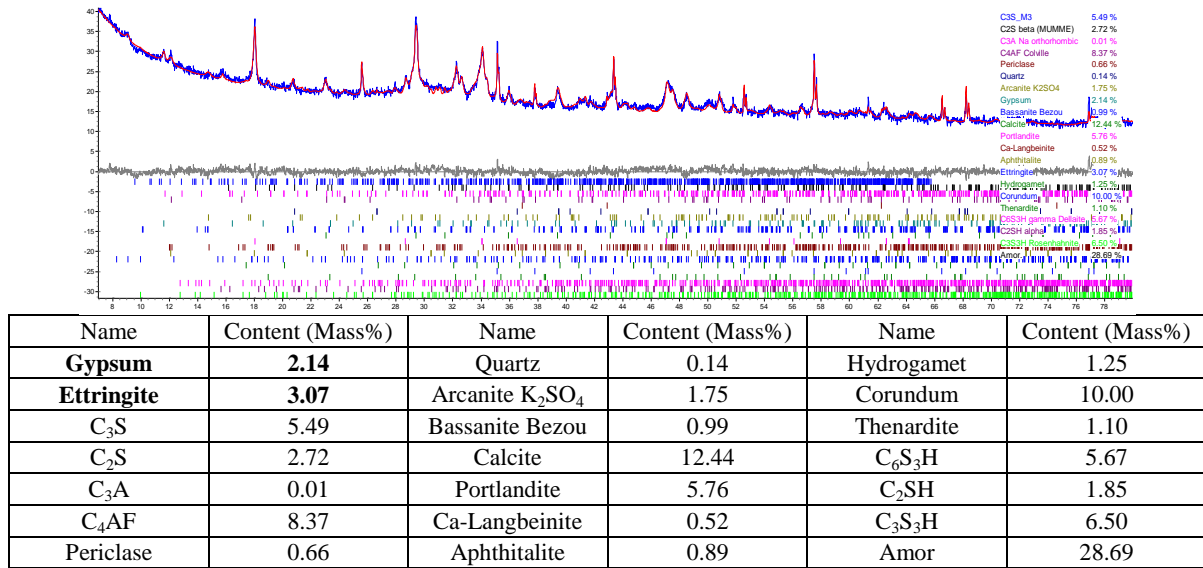
The contents of the gypsum and ettringite formation in the specimens are associated with the surface depth of the specimens, the concentration of  $\text{Na}_2\text{SO}_4$  solution and the corrosion time. Their effects on the gypsum and ettringite

formation are investigated by the powder X-ray diffraction (XRD), and the powder samples for the X-ray diffraction analysis are prepared by the following approach.

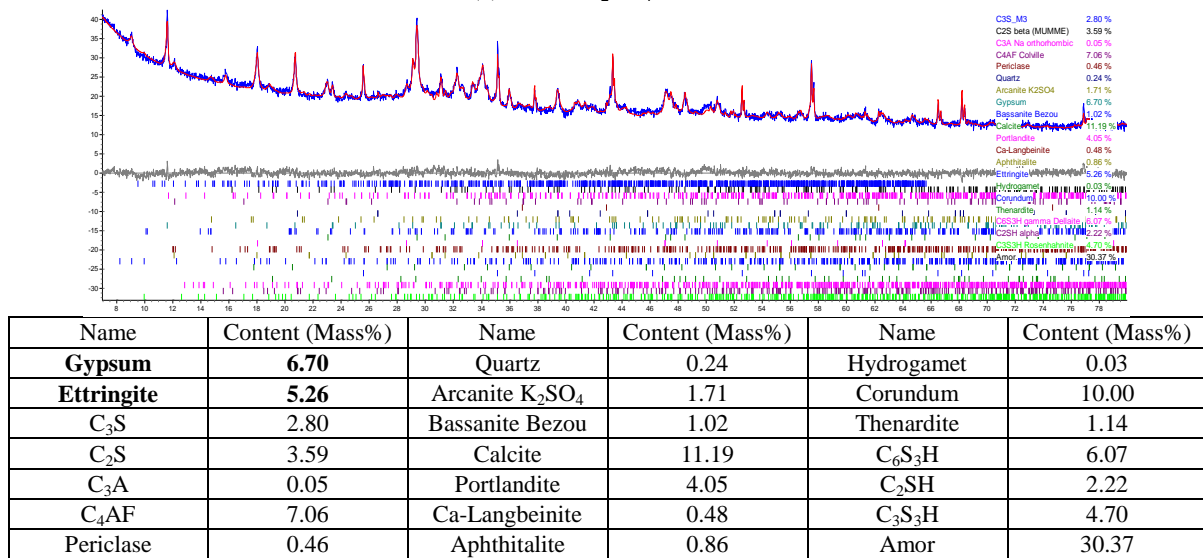
The specimens were removed from the  $\text{Na}_2\text{SO}_4$  solutions every 90 days (87 days in solution), and placed into the vacuum dryer at a temperature of  $50^\circ\text{C}$  for 2 days drying. Immediately, the powders at the surface depth 0-10 mm of the specimens were drilled out according to the six layers: 0-1 mm, 1-2 mm, 2-4 mm, 4-6 mm, 6-8 mm and 8-10 mm while 6-8 drilled points were respectively selected from four exposed surfaces of every specimen. The powders from 6-8 drilled points at the same layer were mixed to pack into a sealing bag, and again placed into the vacuum dryer at a temperature of  $50^\circ\text{C}$  for 1 day drying. After cooling to the room temperature, the powder mixtures were screened by the  $80 \mu\text{m}$  square hole screen, and the screened powders were mixed with the standard  $\alpha\text{-Al}_2\text{O}_3$  powders of less than  $80 \mu\text{m}$  size according to the mass ratio 9:1. This was followed by dropping the anhydrous ethanol into the powders and continues to grind for 1 hour by using an agate mortar and pestle. Finally, all of the powder samples prepared were placed into a vacuum dryer for the powder X-ray diffraction analysis.

### 3.3 X-ray powder diffraction analysis

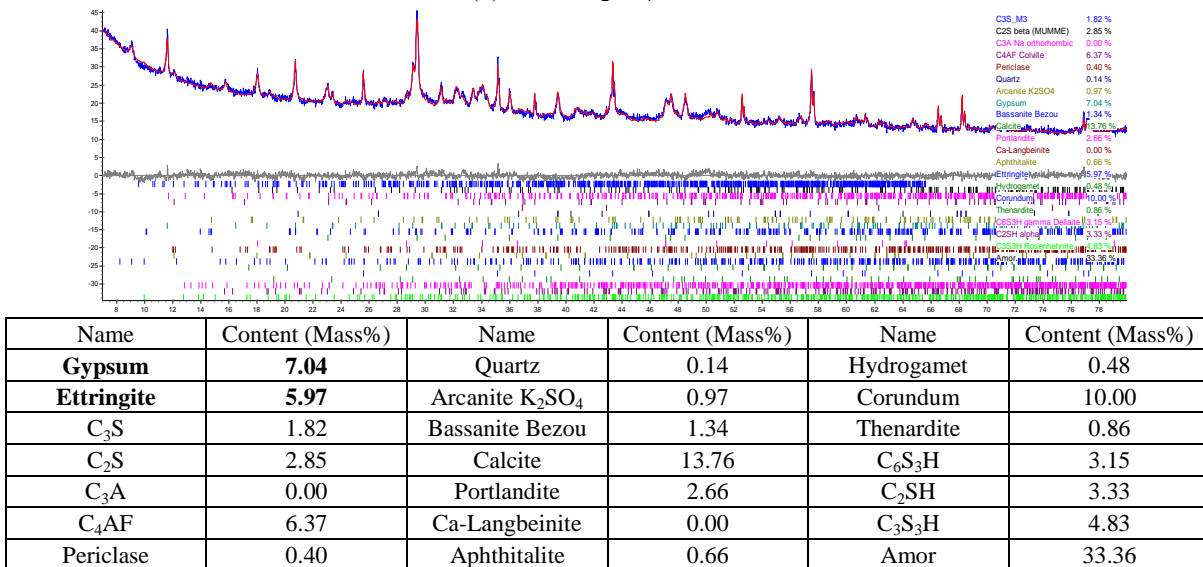
The powder samples were packed into the back-filled



(a) 2.5% Na<sub>2</sub>SO<sub>4</sub> solution



(b) 5.0% Na<sub>2</sub>SO<sub>4</sub> solution



(c) 10.0% Na<sub>2</sub>SO<sub>4</sub> solution

Fig. 5 Comparison between the X-ray diffraction patterns and the quantitative phase analysis results of powder samples from the first layer of specimen under the Na<sub>2</sub>SO<sub>4</sub> solutions for 720 days

Table 2 List of main parameters used in the models

Parameters	Symbol	Value	Equation
Specimen			
Dimensions of specimen	$L_1 \times L_2$ (m×m)	0.04×0.04 (Known)	Eq.(1)
Materials			
Shape factor of hydrated cement particles	$\eta_r$	1.77 (Zuo <i>et al.</i> 2012a)	
Adjustment coefficient	$\omega_{wc}$	1.28 (Zuo <i>et al.</i> 2012a)	Eq.(4)
Cement hydrate degree	$h_a$	0.78 (Known)	
Initial calcium concentration in CSH	$c_{CSH}$ (mol/m <sup>3</sup> )	8126 (Measured by XRD-R)	
Initial calcium concentration in CH	$c_{CH}$ (mol·m <sup>-3</sup> )	4716 (Measured by XRD-R)	
Saturated Ca <sup>2+</sup> concentration in pore	$c_{satu}$ (mol·m <sup>-3</sup> )	21.25 (Nakarai <i>et al.</i> 2006)	Eq.(13)
Calcium ion concentration without CSH	$x_1$ (mol·m <sup>-3</sup> )	2.0 (Nakarai <i>et al.</i> 2006)	
Calcium ion concentration without CH	$x_2$ (mol·m <sup>-3</sup> )	18.25 (Nakarai <i>et al.</i> 2006)	
Initial concentration of calcium aluminates	$c_{CA0}$ (mol·m <sup>-3</sup> )	361.0 (Measured by XRD- R)	Eq.(14)
Environment			
Concentration of sodium sulfate solution	$c_0$ (%)	2.5, 5.0, 10.0 (Known)	Eq.(1)
Environmental temperature	$T$ (°C)	25 (Known)	Eq.(2)
Reaction			
Equivalent reaction coefficient	$q$	3 (Tixier and Mobasher 2003)	Eq.(10)
Reaction rate constant of gypsum	$k_v$ (m <sup>3</sup> ·s <sup>-1</sup> ·mol <sup>-1</sup> )	$3.05 \times 10^{-7}$ (Gospodinov 2005)	Eq.(11)
Reaction rate constant of ettringite	$k_{v1}$ (m <sup>3</sup> ·s <sup>-1</sup> ·mol <sup>-1</sup> )	$1.22 \times 10^{-11}$ (Zuo <i>et al.</i> 2012c)	
Reaction order of calcium aluminates	$\alpha$	1.72 (Zang 1995)	Eq.(14)
Reaction order of gypsum	$\beta$	0.33 (Zang 1995)	

sample holders (to minimise preferred orientation), and measured by a Bruker-Axs D8 DISCOVER X-ray diffractometer with LynxEye Array detector, using Cu target, and operating at a voltage of 40 kV, current of 30 mA and the environmental temperature of 298 K. A soller slit of 4°, a scanning speed of 4°2 $\theta$ /min and a step size of 0.02° 2 $\theta$  were used to examine the samples in the 5°-80° 2 $\theta$  to cover the phases under investigation. Fig. 4 presents only the XRD patterns of the powder samples from the six layers of the specimen when immersed for 720 days into the Na<sub>2</sub>SO<sub>4</sub> solutions.

### 3.4 Rietveld analysis

Considering little of gypsum and ettringite formation in two layers in the specimen depth 6-10 mm, the patterns of powder samples from four layers in the depth 0-6 mm have been selected and further quantitatively analyzed by using the full profile Rietveld method (Scrivener *et al.* 2004, Young 1993), which is implemented in the TOPAS software package (Coelho 2011, Schmidt and Kern 2001). Fig. 5 presents the refined patterns and X-ray diffraction patterns of the powder samples from the 0-1 mm depth of the specimen under 2.5%, 5.0% and 10.0% Na<sub>2</sub>SO<sub>4</sub> solutions for 720 days. It can be seen from the figure that after the Rietveld refinements, the refined patterns approached the X-ray diffraction patterns, and have no residual diffraction peak, so the refined structure models of the powder samples may be used to analyze quantitatively

the contents of gypsum and ettringite in the specimens. The results show that the mass fraction of gypsum and ettringite in the powder samples of the surface layer of the specimen are respectively 2.14%, 6.70%, 7.04% and 3.07%, 5.26%, 5.97% when immersed into 2.5%, 5.0% and 10.0% Na<sub>2</sub>SO<sub>4</sub> solutions for 720 days.

## 4. Comparison between model and experimental results

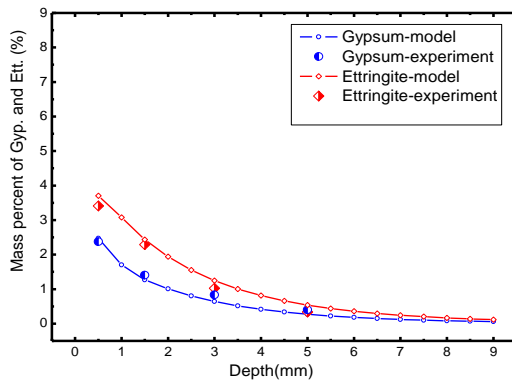
### 4.1 Modeling parameter

In the modelling analysis, the calculation parameters are listed in Table 2.

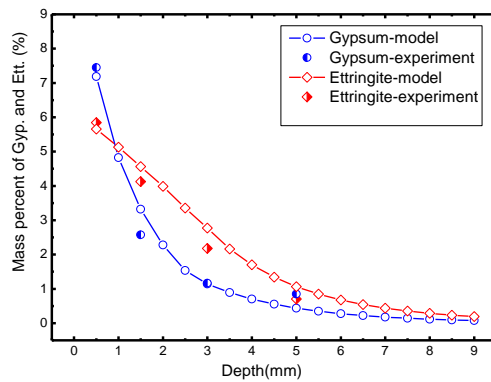
### 4.2 Results and discussion

#### 4.2.1 Effects of surface depth

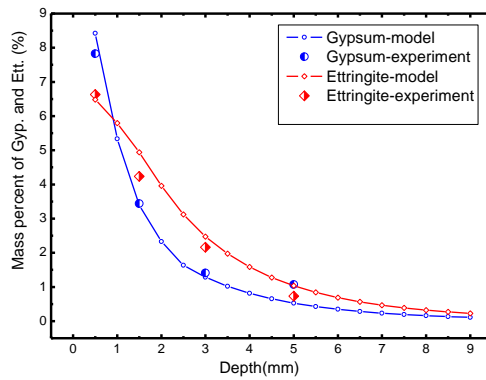
Based on the above models and XRD-Rietveld experiments, the formations of gypsum and ettringite in the cement pastes can be obtained. Fig. 6 presents the mass fraction of gypsum and ettringite formation with the surface depth of the specimens when immersed into Na<sub>2</sub>SO<sub>4</sub> solutions for 20 days. It can be seen from the figures that the formations of gypsum and ettringite are basically within the surface layer 5-mm depth, and decrease with increasing surface depth. Especially in the surface layers 1-4 mm of more volumetric expansion and expansive strain gradient.



(a) 2.5%



(b) 5.0%

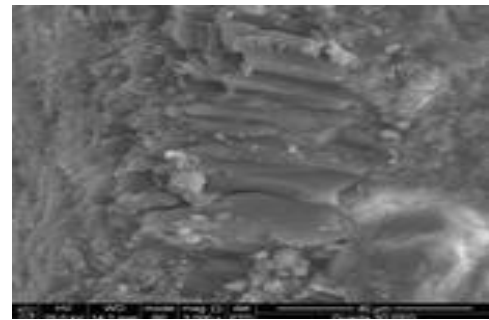


(c) 10.0%

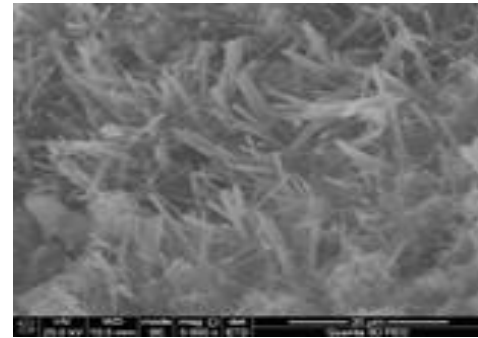
Fig. 6 Formations of gypsum and ettringite with the depth of the specimens immersing into  $\text{Na}_2\text{SO}_4$  solutions for 720 days ( $w/c=0.35$ )

The volume expansion caused by the ettringite formation in the surface layers results in the expansive cracks of cement pastes. Thus, under sulfate attack, the peeling of the surface layer in the specimen is the main characteristics of the damage and failure of cement-based materials (Frank and Raoul 1999, Siad 2013). The quantitative analysis of the gypsum and ettringite formation offers a basis for further analyzing the expansion deformation and damage of cement-based materials subjected to sulfate attack. In addition, Fig. 6 also shows that the formations of gypsum and ettringite obtained by the models are in accordance with the experimental results.

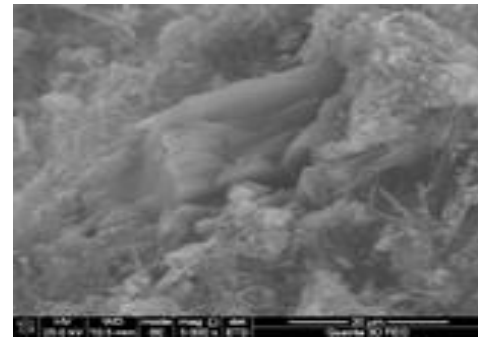
Under the high concentration of  $\text{Na}_2\text{SO}_4$  solutions in Fig. 6(b) and (c), the gypsum formation is more than the ettringite formation in the surface layer 0-1 mm of the



(a) Gypsum in 0-1 mm layer



(b) Ettringite in 3-5 mm layer



(c) Portlandite in 8-10 mm layer

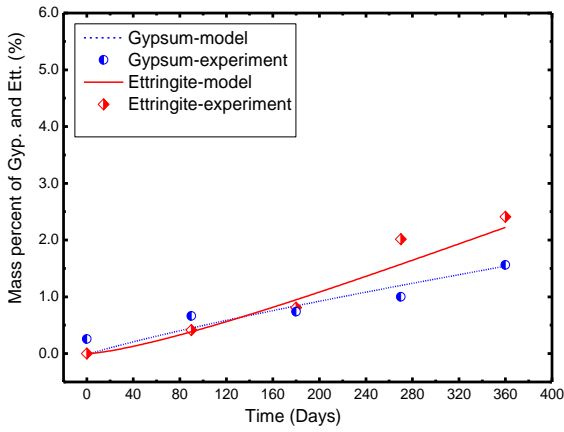
Fig. 7 SEM photograph of specimens in different depths immersed into 5.0%  $\text{Na}_2\text{SO}_4$  solution for 720 days

specimen, but the ettringite formation is greater than the gypsum formation within the surface layer 1-5 mm of the specimen. Fig. 7 presents SEM microscopic morphologies in the surface layers 0-1 mm, 3-5 mm and 8-10 mm of the specimen immersed into 5.0%  $\text{Na}_2\text{SO}_4$  solution for 720 days. It can be observed in the figure that many of plate-shaped gypsum are produced in the surface layer (0-1 mm), while in the middle layer (3-5 mm), a lot of needle-shaped ettringite are observed in the pores. However, in the interior layer (8-10 mm), calcium hydroxide produced by the cement hydration is the main product, and the cement paste in the interior layer of the specimen has not been damaged by sulfate attack during the 720 days.

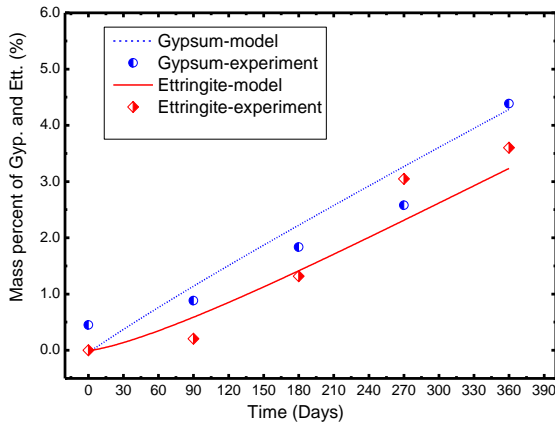
Thus, the modeling and experimental results essentially agree with the observation from SEM micrograph.

#### 4.2.2 Effects of corrosion time

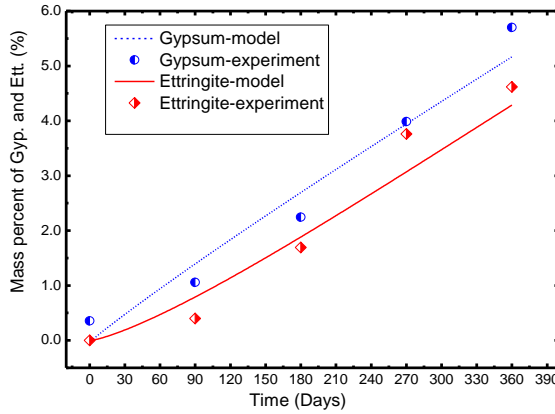
Fig. 8 presents the modeling and experimental results of the gypsum and ettringite formation in the surface layer 0-1 mm with the corrosion time when the specimens are



(a) 2.5%



(b) 5.0%



(c) 10%

Fig. 8 Gypsum and ettringite formation in the surface layer 0-1 mm of the specimens with the corrosion time under different concentrations of  $\text{Na}_2\text{SO}_4$  solutions

immersed into 2.5%, 5.0% and 10.0%  $\text{Na}_2\text{SO}_4$  solutions respectively. It can be seen from the figure that the formations of gypsum and ettringite increase with the corrosion time. During the early days of the corrosion, the formation of gypsum is greater than that of ettringite, but with increasing corrosion time, the concentration of  $\text{Na}_2\text{SO}_4$  solution has an important influence on the gypsum and ettringite formation.

For the specimens immersed into 5.0% and 10.0%  $\text{Na}_2\text{SO}_4$  solutions, as illustrated in Fig. 8(b) and (c), the formation of gypsum is still more than that of ettringite, and

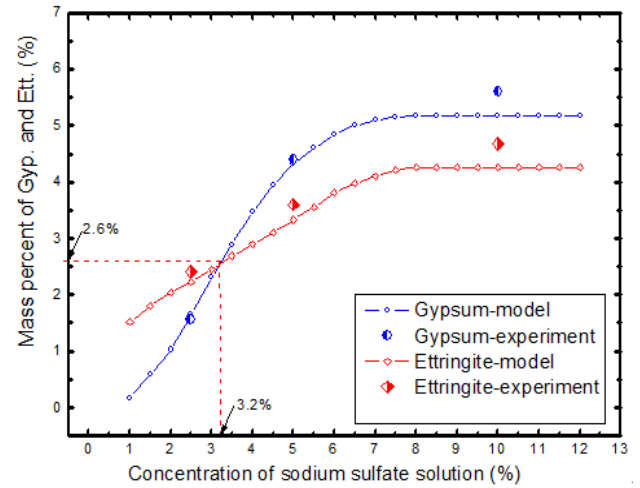


Fig. 9 Effects of concentration of sodium sulfate solution on gypsum and ettringite formation at 360 days

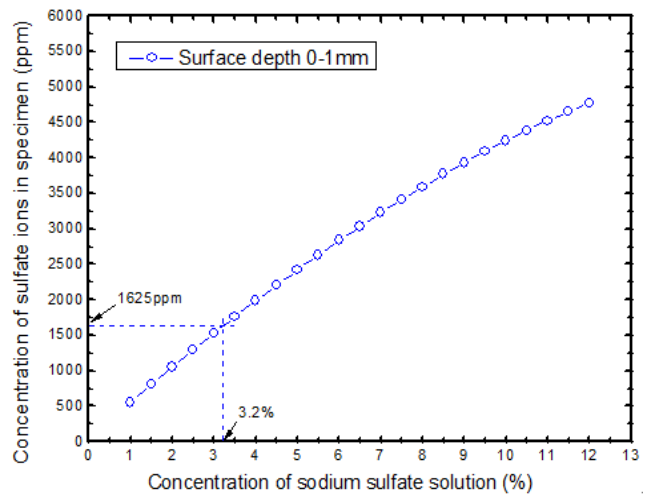


Fig. 10 Numerical results of changes of sulfate ion concentration with solution concentrations at 360 days

the gypsum and ettringite formations increased linearly with the corrosion time, and the increasing rates are basically identical. But for the specimens immersed into 2.5%  $\text{Na}_2\text{SO}_4$  solution, as shown in Fig. 8(a), the formation of ettringite is less than that of gypsum for the first 140 days, and with the increase in the corrosion time, the formation of ettringite increases gradually and faster than that of gypsum, resulting in more formation of gypsum after 140 days. This is because, the diffused sulfate ions firstly react with calcium hydroxide to produce gypsum, and then part of the produced gypsum reacts with the aluminates phases to generate ettringite. At the early stage of sulfate attack, the concentration of sulfate ion in cement pastes is very low, so the formations of gypsum and ettringite in cement pastes are also very slow. But with the increase in corrosion time, the formation of gypsum gradually increases, and the formation rate of ettringite increases with the content of gypsum. In addition, the concentration of  $\text{Na}_2\text{SO}_4$  solution has an important influence on the diffusion and distribution of sulfate ion in cement pastes, and further affects the formation of gypsum and ettringite. Under the lower concentration of  $\text{Na}_2\text{SO}_4$  solution like 2.5%, the distributed

concentration of sulfate ion diffusing into cement pastes is low, so the formation of gypsum and ettringite are slow. But under the high concentration of  $\text{Na}_2\text{SO}_4$  solutions such as 5.0% and 10.0%, the sulfate ion concentration greatly increases, and it accelerates gypsum formation in the cement pastes.

#### 4.2.3 Effects of solution concentration

Fig. 9 presents the contents of the gypsum and ettringite in the depth 0-1 mm of the specimens with the concentrations of  $\text{Na}_2\text{SO}_4$  solution for 360 days immersion. It can be seen from the figure that under the low concentration of  $\text{Na}_2\text{SO}_4$  solutions, the contents of gypsum and ettringite increase with the solution concentration, and the formation of ettringite is greater than that of gypsum in the surface layer. Whereas under the high concentrations of  $\text{Na}_2\text{SO}_4$  solution, the contents of gypsum and ettringite in cement pastes increase slowly, and the formation of ettringite is less than that of gypsum in the surface layer, but when the solution concentration goes up to 6%, the gypsum and ettringite produced in cement pastes increase slowly and tends to be stable.

In the surface layer, the formation of gypsum is less than that of ettringite when the solution concentration is less than 3.2%, and it is greater than the ettringite formation when the solution concentration is greater than 3.2%. With increasing solution concentrations from 1.0% to 6.0%, the formation of gypsum is greater than that of ettringite. The sulfate ion distribution in the specimen has a significant effect on the gypsum and ettringite formation. Using the computing programme NIFGESA.M, numerical simulations on the changes of the distribution concentrations of sulfate ion in the surface depth 0-1 mm with the concentration of  $\text{Na}_2\text{SO}_4$  solutions are described in Fig. 10 when the specimens are immersed for 360 days. It can be obtained from the comparison of Fig. 10 to Fig. 9 that when the gypsum formation is equal to that of ettringite, the mass fraction of which is 2.6%, the distribution concentration of sulfate ion in the surface layer is about 1625 ppm. Further calculation, gypsum and ettringite are established to quantitatively analyze the time- and space-varied formation of gypsum and ettringite in cement pastes subjected to sulfate attack. Furthermore, the experiments on the corrosion of the cement paste specimens with the different concentrations of  $\text{Na}_2\text{SO}_4$  solutions have been performed, and the powder samples from the specimens during the corrosion of  $\text{Na}_2\text{SO}_4$  indicates that, in the different surface depth of the specimen the formations of gypsum and ettringite are basically the same when the sulfate ion concentration of is about 1650 ppm, so the penetrated sulfate ion concentration is an important parameter influencing the gypsum and ettringite formation in cement-based materials.

## 5. Conclusions

The sulfate attack on cement-based materials is a very complicated physical and chemical process associated with the diffusion of sulfate ion, and the formation reactions of the corrosion products such as gypsum and ettringite. This

paper has modeled this process and numerically investigated the formation process of gypsum and ettringite in cement pastes under sulfate attack.

Using the chemical reaction kinetics, in which the second-order reaction between sulfate ions and calcium ions in the pore solution, and the multi-order solid-solid reaction between the gypsum and calcium aluminates in cement pastes are considered, the models for the diffusion-reaction behavior of sulfate ions and the formation process of and solutions were quantitatively analyzed to obtain the time-space-varied formation of gypsum and ettringite in these specimens using X-ray diffraction with the full profile Rietveld method. The results show that the formations of gypsum and ettringite obtained by the proposed models have good agreements with the experimental results, and under the high concentration of  $\text{Na}_2\text{SO}_4$  solutions, gypsum is the main corrosion product in cement pastes, whereas under the low concentration of  $\text{Na}_2\text{SO}_4$  solutions, the main corrosion product is ettringite. However, the numerical investigation of the time- and space-varied formation of gypsum and ettringite helps to model the damage evolution of cement-based materials due to the volume expansion caused by the formation of the corrosion products.

## Acknowledgements

The study of this paper is financially supported by National Science Foundation of China (51378262, 51078186) and by Jiangsu Province Science Foundation (BK20141396).

## References

- Bonen, D. (1992), "Composition and appearance of magnesium silicate hydrate and its relation to deterioration of cement based materials", *J. Am. Ceram. Soc.*, **75**(10), 2904-2906.
- Brown, P., Hooton, R.D. and Clark, B. (2004), "Microstructural changes in concretes with sulfate exposure", *Cem. Concrete Compos.*, **26**(8), 993-999.
- Chandra, A. and Bagchi, B. (1999), "Ion conductance in electrolyte solutions", *Chem. Phys.*, **110**(20), 1024-1034.
- Clifton, J.R., Bentz, D.P. and Pommersheim, J.M. (1994), *Sulfate diffusion in concrete*, NISTIR 5361, Building and Fire Research Laboratory, National Institute of Standards and Technology, Gaithersburg.
- Coelho, A.A., Evans, J.S.O., Evans, I.R., Kern, A. and Parsons, S. (2011), "The TOPAS symbolic computation system", *Powd. Diffr.*, **26**(S1), S22-S25.
- Diamond, S. and Lee, R.J. (1999), "Microstructural alterations associated with sulfate attack in permeable concretes", *J. Am. Ceram. Soc.*, 123-174.
- Frank, R. and Raoul, J. (1999), "The deterioration of mortar in sulphate environments", *Constr. Build. Mater.*, **13**(6), 321-327.
- Garboczi, E.J. (1990), "Permeability, diffusivity, and microstructural parameters: A critical review", *Cement Concrete Res.*, **20**(4), 591-601.
- Gerard, B., Bellego, C.L. and Bernard, O. (2002), "Simplified modelling of calcium leaching of concrete in various environments", *Mater. Struct.*, **35**(254), 632-640.
- Gollop, R.S. and Taylor, H.F.W. (1992), "Microstructural and microanalytical studies of sulfate attack: I. ordinary Portland

- cement paste”, *Cement Concrete Res.*, **22**(6), 1027-1038.
- González, M.A. and Irassar, E.F. (1997), “Ettringite formation in low  $\theta_3\theta$  portland cement exposed to sodium sulfate solution”, *Cement Concrete Res.*, **27**(7), 1061-1072.
- Gospodinov, P.N. (2005), “Numerical simulation of 3D sulfate ion diffusion and liquid push out of the material capillaries in cement composites”, *Cement Concrete Res.*, **35**(3), 520-526.
- Guneyisi, E., Gesoglu, M. and Mermerdas, K. (2010), “Strength deterioration of plain and metakaolin concretes in aggressive sulfate environments”, *J. Mater. Civil Eng.*, **22**(4), 403-407.
- Kalipcilar, I., Mardani-Aghabaglou, A., Sezer, G.I., Altun, S. and Sezer, A. (2016), “Assessment of the effect of sulfate attack on cement stabilized montmorillonite”, *Geomech. Eng.*, **10**(6), 807-826.
- Kamali, S., Moranville, M. and Leclercq, S. (2008), “Material and environmental parameter effects on the leaching of cement pastes: experiments and modeling”, *Cement Concrete Res.*, **38**(4), 575-585.
- Laidler, K.J. (1987), *Chemical Kinetics*, 3rd Edition, Harper and Row Publishers, New York, U.S.A.
- Liu, Z., Deng, D. and Schutter, G.D. (2014), “Does concrete suffer sulfate salt weathering?”, *Constr. Build. Mater.*, **66**(15), 692-701.
- Lothenbach, B., Bary, B., Bescop, P.L., Schmidt, T. and Leterrier, N. (2010), “Sulfate ingress in Portland cement”, *Cement Concrete Res.*, **40**(8), 1211-1225.
- Mainguy, M., Tognazzi, C., Torrenti, J.M. and Adenot, F. (2000), “Modeling of leaching in pure cement paste and mortar”, *Cement Concrete Res.*, **30**(1), 83-90.
- Monteiro, P.J.M. and Kurtis, K.E. (2003), “Time to failure for concrete exposed to severe sulfate attack”, *Cement Concrete Res.*, **33**(7), 987-993.
- Nakarai, K., Ishida, T. and Maekawa, K. (2006), “Modeling of calcium leaching from cement hydrates couples with micro-pore solution formation”, *J. Adv. Concrete Technol.*, **4**(3), 395-407.
- Neville, A. (2004), “The confused world of sulfate attack on concrete”, *Cement Concrete Res.*, **34**(8), 1275-1296.
- Rahman, M.M. and Bassuoni, M.T. (2014), “Thaumasite sulfate attack on concrete: Mechanisms, influential factors and mitigation”, *Constr. Build. Mater.*, **73**(30), 652-662.
- Samson, E.J., Marchand, J., Robert, L. and Bournazel, J.P. (1999), “Modeling ion diffusion mechanisms in porous media”, *J. Numer. Meth. Eng.*, **46**(12), 2043-2060.
- Santhanam, M., Cohen, M.D. and Olek, J. (2003), “Mechanism of sulfate attack: A fresh look Part 2: Proposed mechanisms”, *Cement Concrete Res.*, **33**(3), 341-346.
- Santhanam, M., Cohen, M.D. and Olek, J. (2001), “Sulfate attack research-whither now”, *Cement Concrete Res.*, **31**(6), 845-851.
- Sarkar, S., Mahadevan, S. and Meeussen, J.C.L. (2010), “Numerical simulation of cementitious materials degradation under external sulfate attack”, *Cement Concrete Compos.*, **32**(3), 241-252.
- Sarkar, S., Mahadevan, S., Meeussen, J.C.L., Vander Sloot, H. and Kosson, D.S. (2012), “Sensitivity analysis of damage in cement materials under sulfate attack and calcium leaching”, *J. Mater. Civil Eng.*, **24**(4), 430-440.
- Schmidt, R. and Kern, A. (2001), “Quantitative XRD phase analysis”, *World. Cement*, **32**, 35-42.
- Schmidt, T., Lothenbach, B., Romer, M., Neuenschwander, J. and Scrivener, K.L. (2009), “Physical and microstructural aspects of sulfate attack on ordinary and limestone blended Portland cement”, *Cement Concrete Res.*, **39**(12), 1111-1121.
- Scrivener, K.L., Fullmann, T., Gallucci, E., Walenta, G. and Bermejo, E. (2004), “Quantitative study of Portland cement hydration by X-ray diffraction/Rietveld analysis and independent methods”, *Cement Concrete Res.*, **34**(9), 1541-1547.
- Shazali, M.A., Baluch, M.H. and Al-Gadhib, A.H. (2006), “Predicting residual strength in unsaturated concrete exposed to sulfate attack”, *J. Mater. Civil Eng.*, **18**(3), 343-354.
- Siad, H., Kamali-Bernard, S., Mesbah, H.A., Escadeillas, G., Mouli, M. and Khelafi, H. (2013), “Characterization of the degradation of self-compacting concrete in sodium sulfate environment: Influence of different mineral admixtures”, *Constr. Build. Mater.*, **47**, 1188-1200.
- Sun, W. and Yu, H.F. (2001), *Research Advances on Concrete Durability and Life-time Evaluation*, Forum on Safety and Durability of Civil Structures, China Architecture and Building Press, Beijing.
- Sun, Z.Z. (2005), *Numerical Solutions of Partial Differential Equation*, Science Press, Beijing, China.
- Suresh, A.K. and Ghoroi, C. (2009), “Solid-solid reactions in series: A modeling and experimental Study”, *AICHE. J.*, **55**(9), 2399-2413.
- Tian, B. and Cohen, M.D. (2000), “Expansion of alite paste caused by gypsum formation during sulfate attack”, *J. Mater. Civil Eng.*, **12**(1), 24-25.
- Tixier, R. and Mobasher, B. (2003), “Modeling of damage in cement-based materials subjected to external sulfate attack. I: Formulation, II: Comparison with experiments”, *J. Mater. Civil Eng.*, **15**(4), 305-322.
- Wan, K.S., Li, Y. and Sun, W. (2013), “Experimental and modelling research of the accelerated calcium leaching of cement paste in ammonium nitrate solution”, *Constr. Build. Mater.*, **40**, 832-846.
- Wee, T.H., Zhu, J., Chua, H.T. and Wong, S.F. (2001), “Resistance of blended cement pastes to leaching in distilled water at ambient and higher temperatures”, *ACI Mater. J.*, **98**(2), 184-193.
- Xiong, C., Jiang, L., Zhang, Y. and Chu, H. (2015), “Modeling of damage in cement paste subject to external sulfate attack”, *Comput. Concrete*, **16**(6), 847-864.
- Yang, D.Y., We, S.N. and Tan, Y.Q. (2005), “Performance evaluation of binary blends of Portland cement and fly ash with complex admixture for durable concrete structures”, *Comput. Concrete*, **2**(5), 381-388.
- Yoon, I.S. (2009), “Simple approach to calculate chloride diffusivity of concrete considering carbonation”, *Comput. Concrete*, **6**(1), 1-18.
- Young, J.F. (1998), “Cement-based materials”, *Curr. Opin Solid State Mater. Sci.*, **3**(5), 505-509.
- Young, R.A. (1993), *The Rietveld method*, Oxford University Press, Oxford.
- Zang, Y.R. (1995), *Chemical reaction kinetics*, Nankai university press, Tianjin.
- Zuo, X.B., Sun, W. and Yu, C. (2012b), “Numerical investigation on expansive volume strain in concrete subjected to sulfate attack”, *Constr. Build. Mater.*, **36**(11), 404-410.
- Zuo, X.B., Sun, W., Li, H. and Zhao, Y.K. (2012c), “Modeling of diffusion-reaction behavior of sulfate ion in concrete under sulfate environments”, *Comput. Concrete*, **10**(1), 60-75.
- Zuo, X.B., Sun, W., Li, H. and Zhou, W.J. (2012a), “Geometrical model for tortuosity of transport path in hardened cement pastes”, *Adv. Cement Res.*, **24**(3), 145-154.
- Zuo, X.B., Sun, W., Liu, Z.Y. and Tang, Y.J. (2014), “Numerical investigation on tortuosity of transport path in cement-based materials”, *Comput. Concrete*, **13**(3), 309-323.
- Zuo, X.B., Sun, W., Yu, C. and Wan, X.R. (2010d), “Modeling of ion diffusion coefficient in saturated concrete”, *Comput. Concrete*, **7**(5), 421-435.

